Received: 23 May 2018 | Revised: 3 August 2018 | Accepted: 8 August 2018

DOI: 10.1002/aoc.4581

WILEY Applied Organometallic Chemistry

FULL PAPER

Synthesis and Characterization of VO^{2+}, Co^{2+}, Ni^{2+}, Cu^{2+} and Zn^{2+} Complexes of a Schiff base ligand derived from ethyl 2-amino-6-ethyl-4,5,6,7-tetrahydrothieno[2,3-c] pyridine-3-carboxylate and their Investigation as fungicide Agents

Mohamad M.E. Shakdofa[1,2] | Ammar A. Labib[2] | Naglaa A. Abdel-Hafez[3] | Hanan A. Mousa[2]

[1]Chemistry Department, Faculty of Science and Arts, Khulais, University of Jeddah, Saudi Arabia

[2]Inorganic Chemistry Department, National Research Center, P.O. 12622, Dokki, Cairo, Egypt

[3]Applied Organic Chemistry Department, National Research Center, P.O. 12622, Dokki, Cairo, Egypt

Correspondence
Mohamad M. E. Shakdofa, Chemistry Department, Faculty of Science and Arts, Khulais, University of Jeddah, Saudi Arabia.
Email: mshakdofa@gmail.com;

Ammar A. Labib, Inorganic Chemistry Department, National Research Center, P.O. 12622 Dokki, Cairo, Egypt.
Email: ammar_al@yahoo.com

Complexes of VO^{2+}, Co^{2+}, Ni^{2+}, Cu^{2+}, and Zn^{2+} ethyl-6-ethyl-2-((2-hydroxybenzylidene)amino)-4,5,6,7-tetrahydrothieno[2,3-c]pyridine-3-carboxylate were synthesized and characterized via different spectroscopic techniques. The whole results declared that the complexes assembled in 1:1 mole ratio furthermore, the spectroscopic data analysis proved the present ligand adhered to the different metal ions in neutral or monobasic tridentate ligand via azomethine nitrogen, carbonyl oxygen atoms and protonated/deprotonated phenolic hydroxyl group. The UV–Vis. and ESR spectroscopic data analysis proposed a distorted octahedral or octahedral structure for all complexes. The ESR spectra for Cu^{2+} complexes **(5–6)** revealed an axial symmetry with $g_{\parallel} > g_{\perp} > g_e$, denoting to distorted octahedral Cu^{2+} complex and the free electrons in the M shell exist in a $d_{(x2-y2)}$ orbital with a remarkable covalent bond aspect. The synthesized complexes showed moderate to superb fungicide activity. All complexes are more active than both standard drug and ligand against *C. albicans* where complexes **(5–7)** are more active against *A. flavus* and compounds **(1), (4–5), (7)** against *S. cerevisiae* whereas only complex **(6)** is more active against *A niger*.

KEYWORDS
ESR, fungicide activities, metal complexes, Schiff base

1 | INTRODUCTION

Schiff bases resulted from the condensation of primary amines and carbonyl compounds which discovered by Hugo Schiff in 1894 are structurally recognized as imine or azomethine.[1,2] These possess a vital role in organic, inorganic, medicinal chemistry and biological field owing to their structures; furthermore, these have an imperative role in the theme of coordination chemistry, particularly in the development of complexes owing to its facility to produce stable organo-metal compounds with transition metal ions. Schiff bases and their complexes are versatile extensively used for industrial goals and expose a contrasting broad range of biological activities[3–6] include,

antifungal,[7] antibacterial,[7,8] Anti-leishmanial,[9] anti-molluscicidal,[8] antimalarial,[10] anti-proliferative,[11] anti-inflammatory, antitumor,[12] anti-amoebic,[13] antiviral,[14] antioxidant[15] and antipyretic properties. The Schiff base ligands derived from *o*-vanillin connected with Pd atom forming metal complexes showed a cytotoxic effect on three cancer cell lines: breast (MCF-7), lung (A549) and ovarian (SKOV3).[16] While Cu (II) complexes of Schiff bases of the pyrrolizine-5-carboxamides displayed cytotoxic effect on the breast (MCF-7), ovary (A2780) and colon (HT29) human adenocarcinoma, in addition to MRC5 (normal human fetal lung fibroblast) cells.[17] Niu *et al*. reported that the Zn^{2+} complexes of *o*-vanillin Schiff Bases exhibited efficient DNA interaction and furthermore, showed *in vitro* cytotoxic effect against four different sets of human cancer cell lines (HL-60, HeLa, K562 and A549,).[18] Recently, Venkateswarlu *et al*. stated DNA binding, DNA cleavage, In addition to many other biological studies of Co^{2+} Ni^{2+} and Cu^{2+} complexes with "2-((furan-2-yl) methylimino)methyl)-6-ethoxyphenol Schiff Base,[19] were also carried out. Ghorai *et al*. reported the preparation and characterization of Cu^{2+} and Zn^{2+} complexes of "3-methoxy propylimino) methyl)-6-methoxyphenol" and reported studies related to their capability to DNA binding, DNA cleavage.[20] Numerous of Schiff base complexes show superb catalytic behavior in numerous dissimilar reactions particularly at elevated temperature and in dampness.[21–24]

Due to the above mentioned applications of Schiff bases and in extension of *group preceding work*, on the synthesizing of biologically active metal complexes.[25–28] This work devoted to the preparation of a novel Schiff base ligand, Ethyl 6-ethyl −2 -(2- hydroxylbenzylideneamino)-4,5,6,7-tetrahydrothieno[2,3-c]pyridine-3-carboxylate and its complexes with VO^{2+}, Co^{2+}, Ni^{2+}, Cu^{2+}, and Zn^{2+}. The chemical structure of the recent ligand and metal complexes was investigated by elemental analysis and spectroscopic data. In addition, the fungicide activity for the synthesized complexes was assessed by Well diffusion method.

2 | MATERIALS AND METHODS

All metal salts were purchased from commercial suppliers and used without further purification. Salicylaldehyde was provided from SIGMA-ALDRICH Company as well as DMSO (assay 99.7%) and absolute ethanol (assay ≥99.8%). Ethyl 2-amino-6-ethyl-4,5,6,7-tetrahydrothieno[2,3-c]pyridine-3-carboxylate was prepared according to a known method.[29,30]

3 | INSTRUMENTATION AND MEASUREMENTS

The ligand and its metal complexes were analyzed for C, H, N, and S at the Micro-analytical Laboratory, Cairo University, Egypt. ^{1}H NMR (500 MHz) spectra were recorded in DMSO-d6 on JEOL ECA-500 MHz spectrometer. Chemical shifts (δ) are reported in ppm using TMS as the internal standard. Standard analytical methods were used to determine the metal ion content.[31–34] Mass spectra of the solid ligand and its metal complexes recorded using JEOL JMS-AX-500 mass spectrometer provided with the data system. TLC confirmed the purity of all prepared compounds. IR spectra of the ligand and its metal complexes were measured using a Jasco FT/IR 6100 type A infrared spectrophotometer covering the range 400–4000 cm^{-1}. Nujol mull electronic absorption spectra (EAS) were measured using Whatman filter paper No.1 and referenced against another similar filter paper saturated with paraffin oil in the 200–1100 nm regions on a Shimadzu 2600 spectrophotometer. The thermal analysis (TG) was carried out on Shimadzu DT-50 thermal analyzer from room temperature to 800 °C at a heating rate of 10 °C/min. Magnetic susceptibilities were measured at 25 °C by the Gouy method using mercuric tetrathiocyanatocobaltate (II) as the magnetic susceptibility standard. Diamagnetic corrections were estimated from Pascal's constant. The magnetic moments were calculated from the equation (1):

$$\mu_{eff} = 2.84\sqrt{\chi_M^{corr}}.T \quad (1)$$

Molar conductance was measured on a Tacussel type CD_6NG conductivity bridge using 10^{-3} M DMF solutions. The resistance measured in ohms and the molar conductivities were calculated according to the equation (2):

$$\Lambda_M = \frac{V \times K \times Mw}{g \times \Omega} \quad (2)$$

Where: Λ_M = molar conductivity/ Ω^{-1} cm^2 mol^{-1}, V = volume of the complex solution/mL, K = cell constant (0.92/cm^{-1}), Mw = molecular weight of the complex, g = weight of the complex in gram, Ω= resistance. The solid ESR spectra of the complexes were recorded with Varian E-109 spectrophotometer operating at 9.8 GHz with 100 kHz modulation in CW mode in 3-mm Pyrex tubes at 298 °K. Diphenyl picryl hydrazide (DPPH) used as a g-marker for the calibration of the spectra.

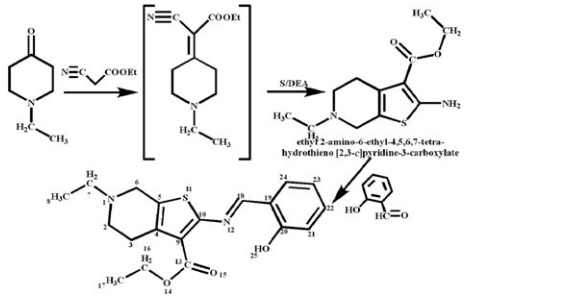

FIGURE 1 Preparation of ethyl-6-ethyl-2-((2-hydroxybenzylidene)amino)-4,5,6,7-tetrahydrothieno[2,3-c] pyridine-3-carboxylate

3.1 | Synthesis of Schiff base (HL)

The ligand, (**HL**) was prepared by refluxing ethanolic solution of ethyl 2-amino-6-ethyl-4,5,6,7-tetrahydrothieno[2,3-c]pyridine-3-carboxylate (254 mg, 1.0 mmol) with ethanolic solution of 2-hydroxy benzaldehyde (122 mg, 1.0 mmol), Figure 1. The mixture stirred and refluxed for three hours, then left to cool to room temperature. The solid product which formed was filtered off, washed with cold ethanol, followed by crystallization from ethanol and finally dried under vacuum over anhydrous $CaCl_2$. The color was yellow and yield 59%. *Elemental microanalyses,* Calc. for ligand **(H_2L)** = $C_{19}H_{22}N_2O_3S$ (FW = 358.45): C, 63.31; H, 5.97; N, 7.56% S, 8.56%. Found: C, 63.66; H, 6.19; N, 7.82%, S, 8.95%. IR data, 3435(br), 1691, 1601, 1560, 1277 cm^{-1} assigned to υ(OH, C=O, C=N, C=C, C-O_{ph}). ^{1}H NMR data (500 MHz, δ ppm DMSO-d_6): 1.06 (3H, t, JHH 6.9,7.60, O–$^{16}CH_2$–^{17}-C**H**$_3$); 1.29 (3H, t, JHH 6.90,7.65, N–$^7CH_2$–^8C***H*****$_3$**); 2.65 (2H, t, N–$^{10}CH_2{}^9C$**H**$_2$); 2.75 (2H, t, N–^{10}C**H**$_2{}^9CH_2$); 3.39 (2H, s, N–^7C**H**$_2{}^8CH_3$); 4.14 (2H, s, N–$^6CH_2$); 4.28 (2H, q, O–$^7CH_2$); 7.65 (1H, d, JHH 7.6, ^{23}C-H); 7.40 (1H, d, JHH 8, 8.05 ^{22}C-***H***); 6.94 (2H, m, $^{3\&4}$C-**H**); 8.76 (1H, s, *N* = ^{18}C-**H**); 12.56 (1H, S, OH). The positive (EI) mass spectrum of ligand showed the parent ion peak at m/z 358(100%) corresponding to (M+) and the following fragments; 301 (45%) $(M\text{-}2CH_3CH_2)^+$, 285.3 (15%) $[M\text{-}2CH_2CH_2\text{-}OH]^+$, 257 (13%) $[M\text{-}2CH_3CH_2\text{-}OH\ \text{-}CHO]^+$, 165 (8%) $[M\text{-}2CH_3CH_2\text{-}OH\text{–}CHO\text{-}C_6H_5]^+$.

3.2 | Preparation of metal complexes (2-7)

The complexes **(2–7)** were prepared by adding metal salts $[VOSO_4]\cdot 2H_2O$, $[Co\ (CH_3COO)_2]\cdot 6H_2O$, $[Ni\ (CH_3COO)_2]\cdot 6H_2O$, $[Cu\ (CH_3COO)_2]\cdot 2H_2O$, $CuBr_2$, $[Zn\ (CH_3COO)_2]\cdot 2H_2O$ (1 mmol, in 30 mL of ethanol) to Ethyl 6-ethyl-2-(2-hydroxybenzylideneamino)-4,5,6,7-tetrahydrothieno[2,3-c]pyridine-3-carboxylate (HL) (358.5 mg, 1 mmol, in 30 ml of absolute ethanol) in the presence of 3 ml of triethylamine except in case of vanadyl complex a 3 ml of distilled water was added. The mixture refluxed for three hours with stirring. The resulting solid complexes filtered off while heated, washed several times with hot ethanol and finally dried over P_4O_{10}.

3.2.1 | VO^{2+}-complex (2)

Yield (61%), m.p. >300 °C; color: green; μ_{eff} = 1.81; molar conductivity (Λ_m): 28.9 $ohm^{-1}cm^2mol^{-1}$. Elemental analysis for $[VO\ (HL)(SO_4)H_2O]\cdot 2H_2O$, $C_{19}H_{24}VS_2N_2O_8$, (559.50): calcd. (Found) %C 40.79(40.48), %H 5.04(4.91), %N 5.01(4.85), %S 5.04(4.91), %V 9.10 (8.79). IR (KBr, cm^{-1}), 3435 ν (H_2O), 1691 ν (C=O), 1602 ν (C=N), 1536 ν (C-$O_{phenolic}$), 1120, 1038 and 727 ν (SO_4), 541 ν (V ← O), 457 ν (V ← N), 984 ν (V=O).

3.2.2 | Co^{2+}-complex (3)

Yield (67%), m.p. >300 °C; color: reddish brown; μ_{eff} = 396; molar conductivity (Λ_m): 14.9 $ohm^{-1}cm^2mol^{-1}$. Elemental analysis for $[Co\ (L)(CH_3COO)(H_2O)_2].5H_2O$, $C_{21}H_{38}NiN_2O_{12}S$, (529.23): calcd. (Found) %C 41.93(41.28), %H 6.37(6.09), %N 4.66 (4.57), %S 5.33(5.29), %Co 9.80(9.67). IR (KBr, cm^{-1}), 3432 ν (H_2O), 1632 ν (C=O), 1596 ν (C=N), 1323 ν (C-$O_{phenolic}$), 1542/1347(Δ= 195) ν (CH_3COO), 541 ν (Co-O), 478 ν (Co ← N).

3.2.3 | Ni^{2+}-complex (4)

Yield (66%), m.p. >300 °C; color: reddish brown; μ_{eff} = 3.11; molar conductivity (Λ_m): 15.5 $ohm^{-1}cm^2mol^{-1}$. Elemental analysis for $[Ni\ (L)(CH_3COO)(H_2O)_2].H_2O$, $C_{21}H_{30}NiN_2O_8S$, (529.23): calcd. (Found) %C 47.66(47.49), %H 5.71(5.51), %N 5.29 (5.36), %S 6.06(5.89), %Ni 11.09(10.85). IR (KBr, cm^{-1}), 3413 ν (H_2O), 1600 ν (C=O), 1585 ν (C=N), 1314 ν (C-$O_{phenolic}$), 1532/1347(Δ= 185) ν (CH_3COO), 531 ν (Ni-O), 499 ν (Ni ← N).

3.2.4 | Cu^{2+}-complex (5)

Yield (58%), m.p. >300 °C; color: deep brown; μ_{eff} = 161; molar conductivity (Λ_m): 35.6 $ohm^{-1}cm^2mol^{-1}$. Elemental analysis for $[Cu\ (HL)Br_2(H_2O)].H_2O$, $C_{21}H_{26}CuN_2O_5SBr_2$, (617.84): calcd. (Found) %C 36.94(36.67), %H 4.24(4.17), %N 4.53 (4.58), %S 5.19 (4.98), %Cu 10.29(10.22). IR (KBr, cm^{-1}), 3418 ν (H_2O), 1611 ν (C=O), 1586 ν (C=N), 1326 ν (C-$O_{phenolic}$), 534 ν (Cu ← O), 442 ν (Cu ← N).

3.2.5 | Cu^{2+}-complex (6)

Yield (53%), m.p. >300 °C; color: brown; μ_{eff} = 1.87; molar conductivity (Λ_m): 11.5 $ohm^{-1}cm^2mol^{-1}$. Elemental analysis for [Cu (L)(CH_3COO)(H_2O)$_2$], $C_{19}H_{28}CuN_2O_7S$, (516.07): calcd. (Found) %C 48.87(48.73), %H 5.47(5.27), %N 5.43 (4.62), %S 6.21(5.99), %Cu 12.31(11.99). IR (KBr, cm^{-1}), 3423 ν (H_2O), 1602 ν (C=O), 1578 ν (C=N), 1353 ν (C-$O_{phenolic}$), 1531/1317(Δ= 214) ν (CH_3COO), 536 ν (Cu-O), 457 ν (Cu ← N).

3.2.6 | Zn^{2+}-complex (7)

Yield (55%), m.p. >300 °C; color: yellow; μ_{eff} = Dia.; molar conductivity (Λ_m): 7.5 $ohm^{-1}cm^2mol^{-1}$. Elemental analysis for [Zn (L)(CH_3COO)].H_2O, $C_{21}H_{26}ZnN_2O_6S$, (499.89): calcd. (Found) %C 50.46(49.93), %H 5.24(5.17), %N 5.60 (5.62), %S 6.41(6.09), %Zn 13.08(12.99). IR (KBr, cm^{-1}), 3400 ν (H_2O), 1642 ν (C=O), 1589 ν (C=N), 1311 ν (C-$O_{phenolic}$), 1555/1355(Δ= 200) ν (CH_3COO), 503 ν (Zn-O), 465 ν (Zn ← N).

3.3 | Biological activity

Well diffusion method used to measure the antifungal activity. Lab. of microbiology, Biology Department, Faculty of Science and Arts, University of Jeddah, KSA.[35–38] Both positive (Amphotericin B) and negative (solvent, DMSO) controls were used in the technique. The complexes and ligand were tested against four fungal strains *Aspergillus niger* (*A. niger*), *Aspergillus flavus (A. flavus), Saccharomyces cerevisiae (S. cerevisiae)* and *Candida albicans* (*C. albicans*) cultured on Czapek Dox's agar as a medium. In a typical procedure, a well was made on the agar medium inoculated with the fungal strains. The well was filled with the test solution (20 mg\ ml) using a micropipette and the plate was incubated at 37 °C for 72 hr. During the test the solution diffused, and the growth of the inoculated fungi or bacteria was affected. The inhibition zone (MIZ) developed on the plate was recorded. Each test took place for three times and the activity index for the complexes was calculated by following formula.[39]

$$\text{Activity index} = \frac{\text{Diameter of inhibition zone by test compound}}{\text{Diameter of inhibition zone by standard}} \times 100$$

4 | RESULTS AND DISCUSSION

The whole attained complexes **(2–7)** are stable in air and have comparable colors, the test of solubility showed that the complexes are water insoluble and soluble in the polar aprotic solvents. Ligand **(1)** Ethyl 6-ethyl-2-(2-hydroxy-benzylideneamino)-4,5,6,7-tetra-hydrothieno[2,3-c]-pyridi-ne-3-carboxylate (HL) was prepared by reaction of salicylaldehyde with 3 Ethyl 2-amino-6-ethyl-4,5,6,7-tetrahydrothieno[2,3-c]pyridine-3-carboxylate in refluxed ethyl alcohol with glacial acetic acid as a catalyst for four hours to give 79% as a yellow solid crystal (Figure 1). The prepared metal compounds had a molar conductivity located within 7.5–35.6 $\Omega^{-1}cm^2mol^{-1}$ range indicating their non-electrolytes nature.[40] The whole spectroscopic analysis and thermal gravimetric data are presented in the experimental part and Tables 1–3**.** The data displayed that all complexes were formed in a molar ratio (1 L:1 M) **(**Figure 2**).**

4.1 | ^{1}H-NMR spectrum

The ^{1}H NMR for the Schiff base, Ethyl −6-ethyl-2-(2-hydroxybenzylideneamino)-4,5,6,7-tetrahydrothieno[2,3-

TABLE 1 The UV–Vis spectra and magnetic moments for the prepared complexes and the parent ligand

No.	π–π*, n–π*, CT and d-d bands	d–d Transition	Geometry	μ_{eff} (BM)
(1)	272, 298, 338, 407	--	--	-
(2)	275, 290, 338, 406, 483, 642, 860	$^2B_2 \rightarrow {}^2E(d_{xy} \rightarrow d_{xz},d_{yz})$ $^2B_2 \rightarrow {}^2B_1(d_{xy} \rightarrow d_{x2-y2})$ $^2B_2 \rightarrow {}^2A_1(d_{xy} \rightarrow d_{z2})$	distorted octahedral	1.81
(3)	273, 296, 338, 384, 404, 485, 509, 1031	$^3T_{2g}(F) \leftarrow {}^3A_{2g}(F)$ $^3T_{1g}(F) \leftarrow {}^3A_{2g}(F)$ $^3T_{1g}(P) \leftarrow {}^3A_{2g}(F)$	octahedral	3.11
(4)	274, 300,339, 386, 454, 539, 1073	$^4T_{2g}(F) \leftarrow {}^4T^{1g}(F)$ $^4A_2(F) \rightarrow {}^4T_1(F)$ $^4T_{1g}(P) \leftarrow {}^4T_{1g}(F)$		3.96
(5)	275, 295, 336, 384, 520, 749, 1099	$^2A_{1g} \leftarrow {}^2B_{1g}$	distorted	1.61
(6)	275, 295, 336, 384, 520, 749, 1099	$^2B_{2g} \leftarrow {}^2B_{1g}$ $^2E_g \leftarrow {}^2B_{1g}$	octahedral	1.87
(7)	270, 300, 340, 410	---		Dia.

TABLE 2 ESR parameters of $VO^{2+}$and Cu^{2+} complexes

Complex No.	(2)	(5)	(6)
$g_{\|\|}$	1.965	2.260	2.258
$g_{\perp}$	2.040	2.057	2.056
g_{iso}	1.99	2.125	2.123
$\mathbf{A_{\|\|} \times 10^{-4}\ (cm^{-1})}$	14.3	137.2	142
$\mathbf{A_{\perp} \times 10^{-4}\ (cm^{-1})}$	96.4	24	14.4
$\mathbf{A_{iso} \times 10^{-4}\ (cm^{-1})}$	69.7	59.4	54.5
$g_{\|\|}/A_{\|\|}$(cm)	-	164.7	158.6
G	-	4.56	4.64
ΔE_{xy} (cm^{-1})		13717	14684
ΔE_{xz} (cm^{-1})	-	19230	21786
$K_{\|\|}^2$	-	0.534	0.567
$K_{\perp}^2$	-	0.636	0.70
K^2	-	0.602	0.658
K	--	0.776	0.81
α^2	0.415	0.702	0.714
β^2	0.959	0.76	0.79
γ	-	0.91	0.98

[a]$g_{iso} = (2g_{\perp}+g_{\|})/3$ [b] $G = (g_{\|}-2)/(g_{\perp}- 2)$.

c]pyridine-3-carboxylate (HL) was measured in DMSO-d_6. ^{1}H-NMR spectrum for the ligand (**1**) **(**Figure 3**)** displayed a peak of hydroxyl proton at δ = 12.56 ppm.

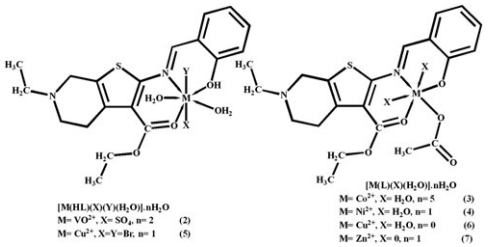

FIGURE 2 Structure representation of metal complexes (2-7)

This hydrogen chemical shift observed at high values of δ characteristic to their bonding to the oxygen atom that is lean to electronegativity in nature. This consequence was confirmed by the signal chart of the prepared ligand which showed that the notable decrease of the strength of the signals (Figure 4**).** While the azomethine proton *H*-^{18}C=N appeared as the singlet at δ = 8.76 ppm. The aromatic protons H-$C^{21\&24}$ can be observed as a doublet at δ = 7.65 and 7.40 ppm with JHH equal to 7.6 and 8 & 8.05 consecutively while the aromatic protons *H*-$C^{22\&23}$ appeared as multiple at 6.94.

4.2 | Mass spectrum

The spectrum of mass MS for the ligand (**1**) proof the suggested chemical structure for the molecular ion peak m/z equal 358 (100%) **(**Figure 5**)**. Furthermore, many fragments can be observed at 343, 329, 315, 301, 285 and

TABLE 3 Thermogravimetric data of Schiff base complexes (2-7)

	Temp. range (°C)	Loss in weight Found (calcd.)	assignment	Composition of the residue
(2)	30–100	6.50 (6.88)	Dehydration process ($2H_2O$)	[VO (HL)(SO_4)(H_2O)]
	100–170	3.7 (3.44)	Loss of coordinated water molecule	[VO (HL)(SO_4)]
	245–260	17.76 (18.34)	Loss of one sulphate ion (H_2SO_4)	[VO (HL)]
	260–490	63.63 (53.97)	Complex decomposition forming V_2O_5	V_2O_5
(3)	50–95	14.89 (14.97)	Dehydration process ($5H_2O$)	[Co (L)(CH_3COO) $H_2O)_2$]
	115–200	5.67 (5.99)	Loss of two coordinated water molecule	[Co (L)(CH_3COO)]
	200–235	9.51 (9.88)	Loss of one acetate ion (CH_3COOH)	[Co (L)]
	390–515	58.55 (56.70)	Complex decomposition forming CoO	CoO
(4)	40–100	3.13 (3.4)	Dehydration process (H_2O)	[Ni (L)(CH_3COO)($H_2O)_2$]
	110–190	6.61 (6.81)	Loss of two coordinated water molecules	[Ni (L)(CH_3COO)]
	240–265	11.08 (11.23)	Loss of one acetate ion (CH_3COOH)	[Ni (L)]
	350–480	65.77 (64.44)	Complex decomposition forming NiO	NiO
(5)	40–90	2.79 (2.92)	Dehydration process ($2H_2O$)	[Cu (HL)Br_2(H_2O)]
	110–150	3.03 (2.92)	Loss of coordinated water molecule	[Cu (HL)Br_2]
	230–255	24.88 (25.78)	Loss of two bromide ions (2HBr)	[Cu (HL)]
	350–450	57.10 (55.43)	Complex decomposition forming CuO	CuO
	100–170	6.58 (6.98)	Loss of two coordinated water molecules	[Cu (L)(CH3COO)]
(6)	210–230	11.63 (11.5)	Loss of one acetate ion (CH3COOH)	[Cu (L)]
	370–470	68.23 (66.09)	Complex decomposition forming CuO	CuO
(7)	30–60	4.1 (3.60)	Dehydration process (H_2O)	[Zn (L)(CH_3COO)]
	220–271	11.39 (11.89)	Loss of one acetate ion (CH_3COOH)	[Zn (L)]
	275–375	67.57 (68.22)	Complex decomposition forming ZnO	ZnO

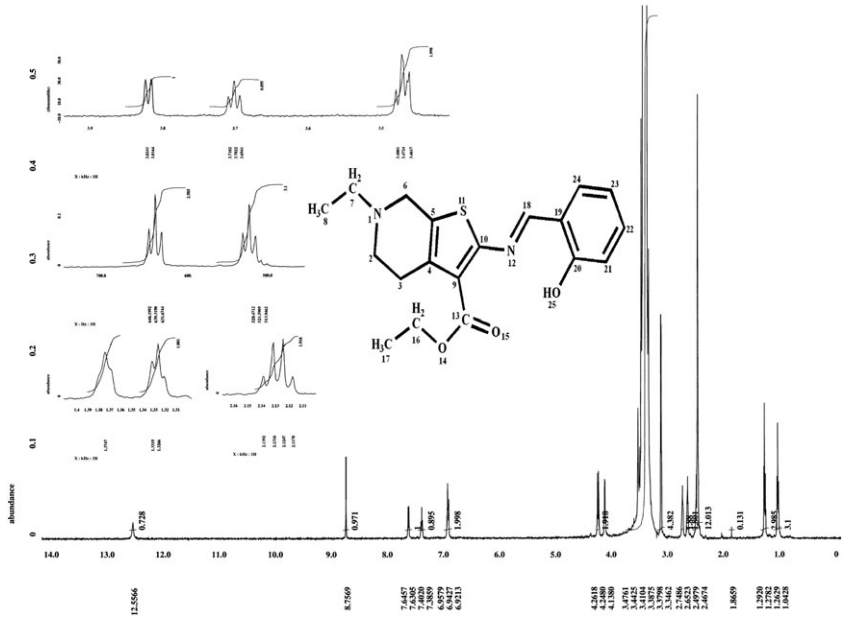

FIGURE 3 The ^{1}HNMR spectrum of the Schiff base (1)

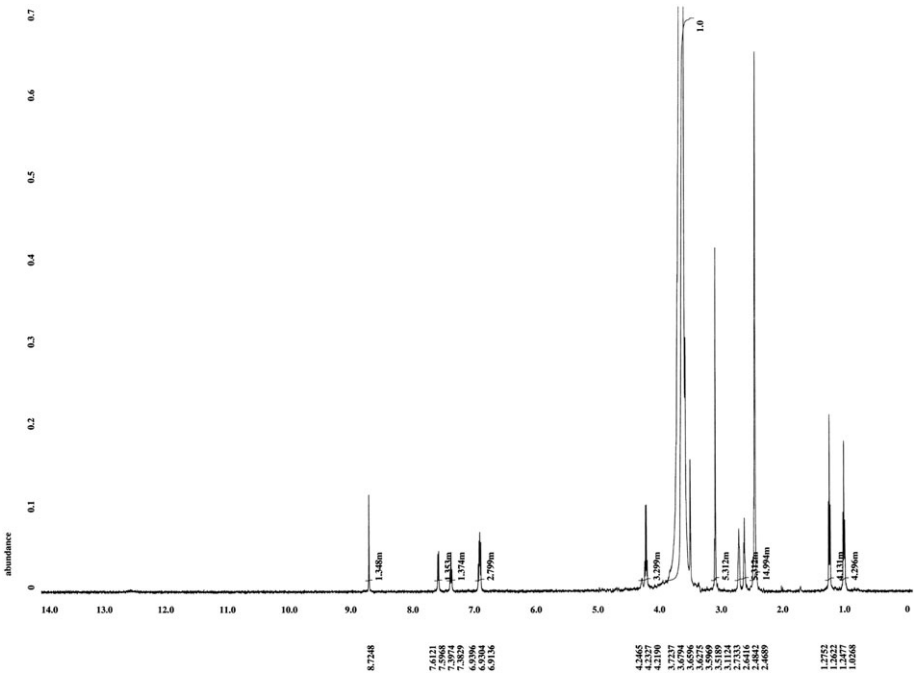

FIGURE 4 The Deuterated ^{1}HNMR spectrum of the Schiff base (1)

255 owing to the loss of methyl, ethyl and finally carboxylic group. In addition, there are main fragments appeared at m/z 238 belong to fragment ethyl 6-ethyl-4,5,6,7-tetrahydro-[2,3-c]-thieno[5,4-c]pyridine-3-carboxylate, the second peak at m/z = 121 owing to the presence of fragment 2-(iminomethyl)phenol. The peaks at m/z = 135, 105, 94, 77 expected to be for fragment 4,7-dihydrothieno[2,3-c] pyridine, phenylmethanimine, phenol and benzene respectively.

4.3 | IR spectra

The data of infrared spectra of the Schiff base (**1**) displayed a broad band at 3435 cm^{-1} and a band at 1278 which ascribed to the hydroxyl and C-OH of phenolic moiety. The carbonyl group ν(C=O) of carboxylate moiety was detected at 1692 cm^{-1}, while the azomethine group ν(C=N) appeared at 1602 cm^{-1}. The manner of chelation can be recognized by matching the IR spectrum

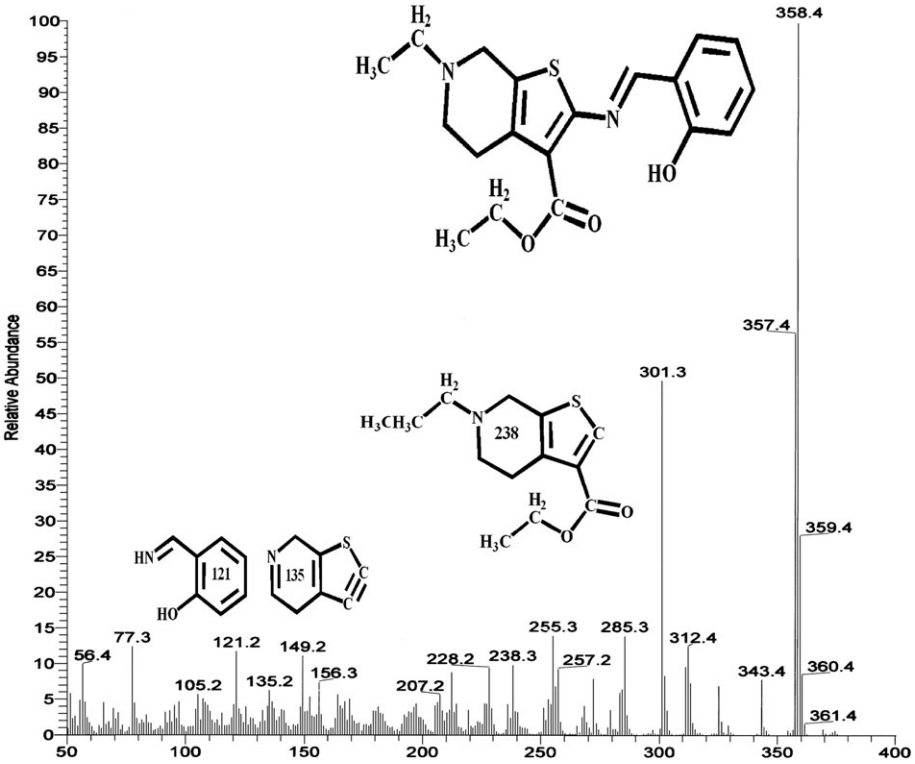

FIGURE 5 Mass spectrum of the Schiff base (1)

of the complexes with the original IR spectrum of Schiff base **(1)**. The matching clear that the Schiff base **(1)** works either as:

1. **Neutral tridentate** ligand chelated to the VO^{2+} and Cu^{2+} ion via the azomethine (N atom), and the protonated hydroxyl group (O atom) of phenolic moieties as in complexes **(2)** and **(5)**. This type of coordination was recommended by four pieces of evidences as follow:
2.
   i. The shift toward the negative of the υ (OH) group and the positive shift of phenolic C-OH proof the contribution of the hydroxyl group.
   ii. The azomethine group showed a shift towards negative in both position and intensity, valued by 16 and 46 cm^{-1} consecutively.[41–44]
   iii. The carbonyl group showed a shift towards negative in both position and intensity, valued by 28 and 80 cm^{-1} consecutively.
   iv. The existence of new bands at 541, 534 and 457, 442 cm^{-1} for complexes **(2)** and **(5)** can be signified to the ν(M ← O) and ν(M ← N) consecutively.[45]

3. **Monobasic tridentate ligand**, forming a covalent bond by the (O atom) of deprotonated hydroxyl group of phenolic moieties and coordinated via azomethine (N atom) and carbonyl (O atom) groups as found in complexes **(3–4)** and **(6–7)**. This type of coordination was recommended by four pieces of evidences as follow:
   i. The misplaced of ν(OH) band signifying the engagement of the deprotonated phenolic hydroxyl group which was confirmed by the positive shift in the position of the phenolic C-O band.
   ii. The azomethine group shows a negative shift in both location and intensity for (C=N) groups by 17–42 cm^{-1}, respectively.
   iii. The carbonyl group in the azomethine showed a negative shift in both location and intensity by (41–91 cm^{-1}).
   iv. The existence of IR bands located at the ranges 503–541 and 457–499 cm^{-1} for the prepared complexes can be ascribe to the ν(M–O) and ν(M ← N) consecutively.[45]

In case of VO^{2+} complex, a recent band signal appeared at 984 cm^{-1}, that ascribed to ν(V=O).[46] The presence of two new bands in the acetate complexes **(3–4)** and **(6–7)** in the 1531–1555 and 1339–1351 cm^{-1} are imputing to both the symmetric and asymmetric stretching band vibration of the acetate ion [(ν_{as} (COO^-) and ν_s (COO^-))]. The difference values (Δ) between ν_{as} (COO^-) and ν_s (COO^-) in **(3–4)** and **(6–7)** were in range 183–206 cm^{-1} implying to mono-chelated acetate

group.[47–49] The sulfate complex **(2)** demonstrated bands at 1120, 1038 and 727 cm^{-1} distinctive for the mono-chelated sulfate group, where the low conductance values of the compounds affirmed the later state.[25,47]

4.4 | Electronic Absorption Spectra of the prepared complexes and parent ligand

The EAS of the compounds are outlined in Table 1. The UV–Vis. spectrum of Schiff base **(1)** demonstrated, three absorption bands at 272, 298, 338 nm because of the intra-ligand π-π* transition in the benzenoid moiety that nearly unchanged on chelation and n → π* transitions of the azomethine and carbonyl groups.[50,51] The bathochromic shift of these absorption bands on chelation may be owing to the participation of a lone pair of electrons of N and O atoms to the metal ion, demonstrating the participation of azomethine and carbonyl groups in chelation.[52] Additionally, the band at 407 nm may be assigned to the transition within the molecule, actually an intramolecular charge transfer interaction.[52,53] The VO^{2+} complex UV–Vis. spectrum demonstrated three beaks located at 860, 642 and 483 nm, attributed to the electronic transition "$^2B_2 \rightarrow {}^2E(d_{xy} \rightarrow d_{xz}, d_{yz})$, $^2B_2 \rightarrow {}^2B_1(d_{xy} \rightarrow d_{x2-y2})$ and $^2B_2 \rightarrow {}^2A_1(d_{xy} \rightarrow d_{z2})$" (Table 1) which are harmonious to an octahedral skeletal for VO^{2+}complexes (Figure 2).[54–57] However, the Co^{2+} complex **(3)** spectrum demonstrated three bands at 1073, 539 and 454 nm which is ascribable to "$^4T_{2g}(F) \leftarrow {}^4T^{1g}(F)$, $^4A_2(F) \rightarrow {}^4T_1(F)$ and $^4T_{1g}(P) \leftarrow {}^4T_{1g}(F)$" transition in octahedral ligand field.[56] The UV–Vis. spectrum for Ni^{2+} complex demonstrated three peaks originates at 1031, 539 and 485 that ascribable to electronic transitions "$^3T_{2g}(F) \leftarrow {}^3A_{2g}(F)$, $^3T_{1g}(F) \leftarrow {}^3A_{2g}(F)$ and $^3T_{1g}(P) \leftarrow {}^3A_{2g}(F)$" which are compatible with a Ni^{2+}ion in an octahedral skeletal (Figure 2).[56,58] The UV–Vis. spectra of Cu^{2+} complexes **(5)** and **(6)** demonstrated three bands originates at 1083, 749 and 520 nm and 1068, 681, 459 nm consecutively which are ascribable to electronic transitions "$^2A_{1g} \leftarrow {}^2B_{1g}$, $^2B_{2g} \leftarrow {}^2B_{1g}$, $^2E_g \leftarrow {}^2B_{1g}$" denoting the complexes has a strong tetragonal distorted octahedral geometry around metal ion **(**Figure 2**)**.[56]

4.5 | Magnetic moment (μ_{eff}) measurements

The μ_{eff} data of polycrystalline metal complexes at 298 °K are shown in Table 1. The data showed that VO^{2+}, Co^{2+}, Ni^{2+} and Cu^{2+} are paramagnetic but Zn^{2+} is diamagnetic. The μ_{eff} for VO^{2+} and Cu^{2+}complexes (**2**) and **(5–6**) were found to have values lying between 1.61 to 1.87 BM corresponding to one unpaired electron system (1.73 BM).[59] The μ_{eff} values for Co^{2+} and Ni^{2+} complexes (**3**) and **(4)** are equal to 3.11 and 3.96 BM consecutively, which confirmed electronic configuration with two and three unpaired electrons in an octahedral environment.[60,61]

4.6 | ESR spectra of VO^{2+} and Cu^{2+} complexes

The ESR spectra for VO^{2+} and Cu^{2+} complexes provide more information about their geometry. The compounds were recorded on ESR at 9.8 GHz in polycrystalline state at 25 °C Table 2.The ESR of VO^{2+} complex (d^1, ^{51}V, $I = 7/2$) shows axially anisotropic spectrum with eight line investigating to $g_\perp > g_{||}$and $A_{||} > A_\perp$relationship, this is true for a distorted octagonal structure that refers to the d_{xy} ground state.[62] It demonstrates two sets of resonance components, due to the parallel ($g_{||}$) and perpendicular ($g_\perp$) features which a signifying to axially symmetric anisotropy. These data demonstrating that there is an interaction between the spin of both vanadium nucleus and electron. The super-hyperfine splitting of nitrogen atom does not appear on vanadium signals, demonstrating that the interactive happens between the spin of electron and ligand.[63] Such values are demonstrating that the VO^{2+} has a deformed octahedral structure.[55,64] The α^2 and β^2 (molecular orbital coefficient) of VO^{2+} complex were evaluated utilized the subsequent equations.[54]

$$\alpha^2 = \frac{(2.0023 - g_{||})E}{8\lambda\beta^2}$$

$$\beta^2 = 1.17\left(-\frac{A_{||}}{P}\right) + \left(\frac{A_\perp}{P}\right) + (g_{||} - 0.36g_\perp) - 0.64g_e$$

"where $P = 128 \times 10^{-4}$ cm^{-1}, $\lambda = 135$ cm^{-1} and E is the electronic transition energy of $^2B_2 \rightarrow {}^2E$". The higher value for β^2 with respect to α^2 denoted that in-plane π-bonding is less covalent than in-plane σ-bonding.[54,65] The β^2 (in-plane π-bonding parameter) value is compatible with the data of VO^{2+} complexes of acetyl acetone and Schiff base published by Walter, Patron McGarvey, Dodwad and Raman.[64–68]

The Cu^{2+}-complexes **(5–6)** ESR spectra displayed that the complexes demonstrate anisotropic signals with $g_{||}$ (2.260, 2.258), $g_\perp$(2.057, 2.056) and g_{iso} (2,124, 2,123) values which are distinguishing to a types with a d^9 arrangement and having an axial symmetry specie of a $d_{(x2-y2)}$ ground state, that is recognized for Cu^{2+} complexes.[39,69] This g-values support that the Cu^{2+}-complexes **(5–6)** adopted an octahedral or square-planar geometry.[70,71] The ESR data shows $g_{||} > g_\perp > 2.0023$, signifying that the structure around the Cu^{2+} ion are deformed.[72] The term G is related to g-values "G =

$(g_{||}\text{-}2)/(g_{\perp}\text{-}2)$".[73] If G < 4.0, significantly the exchange coupling is present, if G > 4.0, thus domestic tetragonal axes are align parallel or only partially misalign. Cu^{2+}-complexes **(5–6)** demonstrate G equal to 4.56 and 4.64, signifying the occurrence of tetragonal axes. In addition, the value of $g_{||}/A_{||}$can be used as a diagnostic of stereochemistry.[74] If the value ranged from 105 to 135 the geometry is square-planar while if it is ranged from 150 to 250 the geometry is tetrahedrally distorted octahedral 150–250 cm^{-1}. The $g_{||}/A_{||}$for complexes **(5–6)** are 164.7 and 158.6 confirmed that the geometry of Cu^{2+} complexes **(5–6)** are tetragonally distorted octahedral.[48,73] Kivelson and Neiman display that for the Cu^{2+}-complexes the $g_{||}$-valuable can be utilized to depict the metal–ligand bond aspect. If the $g_{||}$-valuable is larger than 2.3 the environmental is principally ionic while if it is smaller than 2.3 the environmental is principally covalent.[75] For Cu^{2+} complexes **(5–6)** the $g_{||}$-values are 2.260 and 2.258 which signify that the bonds are principally covalent bonds.[74] The g-values could be concerned to the parallel ($k_{||}$) and perpendicular ($k_{\perp}$) parts of the orbital reduction factor (k) as in these equations.[76–79]

$$k_{\parallel}{}^2 = \left(g_{\parallel} - 2.0023\right)\ \Delta Exy/8\lambda^{\circ}$$

$$k_{\perp}{}^2 = \left(g_{\parallel} - 2.0023\right)\ \Delta Exz/2\lambda^{\circ}$$

$$= \left(k_{\parallel}{}^2 + 2k_{\perp}{}^2\right)/3$$

"Where λ_o is free Cu^{2+} ion for the spin orbit coupling (-828 cm^{-1}) ΔE_{xy} and ΔE_{xz} are the electronic transitions $^2B_{1g} \rightarrow {}^2E_g$ and $^2B_{1g} \rightarrow {}^2B_{2g}$ consecutively". The calculating values of $k_{||}{}^2$, $k_{\perp}{}^2$ and k^2 demonstrated that $k_{||}{}^2 < k^2$ supporting that the ground state for complexes **(5–6)** is $^2B_1$. Additionally, when the environmental is covalent, k < 1 but if more than 1 the environmental is ionic. The k value for complexes **(5–6)** are 0.776 and 0.810 consecutively which are smaller than the unity denoting the covalency nature of the environmental that agrees with the data given by the $g_{||}$-values.[78–80]

The α^2 (in-plane sigma bonding parameters) valuable could be assessed by the subsequent equations.[39,71]

$$\alpha^2 = \left(g_{\parallel} - 2.0023\right) + \frac{3}{7}(g_{\perp} - 2.0023) - \left(\frac{A_{\parallel}}{P}\right) + 0.04$$

"Where P is the free ion dipole expression equal 0.036". If α^2 equal to 1, the bond could be pure ionic but if it is equal to 0.5, the bond could be pure covalent, assumption that $P = 0.036\ cm^{-1}$ and K = 0.43.[39,71] The Cu^{2+}-complexes **(5–6)** α^2 values are 0.702 and 0.714 suggesting the covalency nature of in-plane sigma bonding.[81] The γand βcoefficients (out-of-plane and in-plane π-bonding) can be could be assessed utilized the subsequent equations.[76]

$$\alpha^2\gamma^2 = K_{\perp}{}^2$$
$$\alpha^2\beta^2 = K_{\parallel}{}^2$$

The Cu^{2+} complexes **(5–6)** γ^2 values are 0.91 and 0.98 while the β^2 values are 0.76 and 0.79 consecutively, suggesting the covalency nature of out-of-plane and in-plane π-bonding.[48,76]

4.7 | Thermal analysis

To attain additional informative data concerned with the stability and nature of water molecules in the complexes, the TG analysis for **(2–7)** scanned in the temperatures 25 to 800 °C. The data of thermo-analysis are cited in Table 3 and demonstrated that there is a clear correspondence between the weight loss of the calculating and proposed formulae. These are signified that the **(2–7)** are generally decayed in three or four phases that could be understood as follows:

1. The dehydration process occurs through 30–100 °C accompanied by weight loss ranged from 2.79(2.92) to 14.89(14.97) % matching to the evolution of one, two or five water molecules as in complexes **(2–5)** and **(7)**.
2. The second phase appears in **(2–6)** occur at 100 and 200 °C with losing in weight ranged from 3.03(2.92) to 6.58(6.98) % which ascribed to the excluding of the chelated water molecules.
3. The anions (sulfate, bromide or acetate) eliminated from the complexes at temperature range 200 to 271 °C with weight lose 9.51(9.88) to 24.88(25.78) %.
4. Finally, the complete disintegration of the complexes through the oxidation of the organic part occur through 260–515 °C range forming metal oxide.

4.8 | Biological activity

Fungicide activity of the compounds was assessed by Well Diffusion technique against *A. niger*, *A. flavus, S. cerevisiae* and *C. albicans*. The screening data (Table 4) showed that the activity of the parent Schiff base-(**1**) equal or more than *Amphotericin B* against *C. albicans* and *S. cerevisiae* within inhibition zone, (MIZ, mm)/activity index (AI%) equal to 14(100) and 23(104.5). while the parent Schiff base-(**1**) activity against *A. niger*, *A. flavus*, is less than *Amphotericin B*. Some complexes were more effective than both Amphotericin *B* and the parent Schiff base-(**1**). The most biologically active compounds against *A. niger* is complex **(6)** with MIZ equal to 20 (AI 117.6),

TABLE 4 Antifungal activities of ligand and its complexes against *A. niger, A. Flavus, S. cerevisiae and C. albicans*

	A. niger		A. flavus		S. cerevisiae		C. albicans	
Compound No.	inhibition zone (mm)	Activity Index (%)	inhibition zone (mm)	Activity Index (%)	inhibition zone (mm)	Activity Index (%)	inhibition zone (mm)	Activity Index (%)
Amphotericin B	17	100	19	100	22	100	14	100
Ligand	14	82.4	14	73.7	23	104.5	14	100
(2)	11	64.7	19	100	21	95.5	16	114.3
(3)	14	82.4	13	68.4	17	77.3	16	114.2
(4)	13	76.5	15	78.9	30	136.3	15	107.1
(5)	15	88.2	28	147.4	25	113.6	20	142.9
(6)	20	117.6	26	136.8	15	68.2	24	171.4
(7)	16	94.1	30	157.9	29	131.8	21	150

complex **(7)** against *A. Falvus with* MIZ equal to 30 (AI 157.9), complex **(4)** against *S. cerevisiae with* MIZ equal to 30 (AI 136.3), and complex **(6)** against *C. albicans* with MIZ equal to 24 mm (AI 171). The rest complexes showed a medium activity against the four species with MIZ in the ranges of 11–16 mm (AI 64.7–94.1), 13–28 mm (AI 68.4–147.4), 15–29 mm (AI 68.2–131.8) and 15–21 mm (AI 107.1–150). The activity order is sorted in Figure 6. The high biological activity of the prepared complexes may attribute to the central metal ion lipophilicity that build on the bases of Overtone's concept and Tweedy's chelation theory. In conventionality with Overtone's concept of cell permeability, the lipophilic soluble complexes can traverse across the cell membrane, so the lipo-solubility are consisting a fundamental factor that affect the antimicrobial activity. On chelation, the polarity of metal ion become remarkably more restrictive due to the obstructing of the orbital in the ligand, along with the engagement of the positive charge of the metal ion partially with donor atoms. Additionally, this encourages the allocation of π-electrons across the chelating ring and this fundamentally increases the complexes lipophilicity, which leading to raising the capability of the complexes to penetrate the membranes of the lipid and hinder the metal binding sites of the cell enzymes. The synthesized complexes also break down the respiratory operation of the cells, which lead to the generation of the proteins, and intercept microbe cells growth.[82–84]

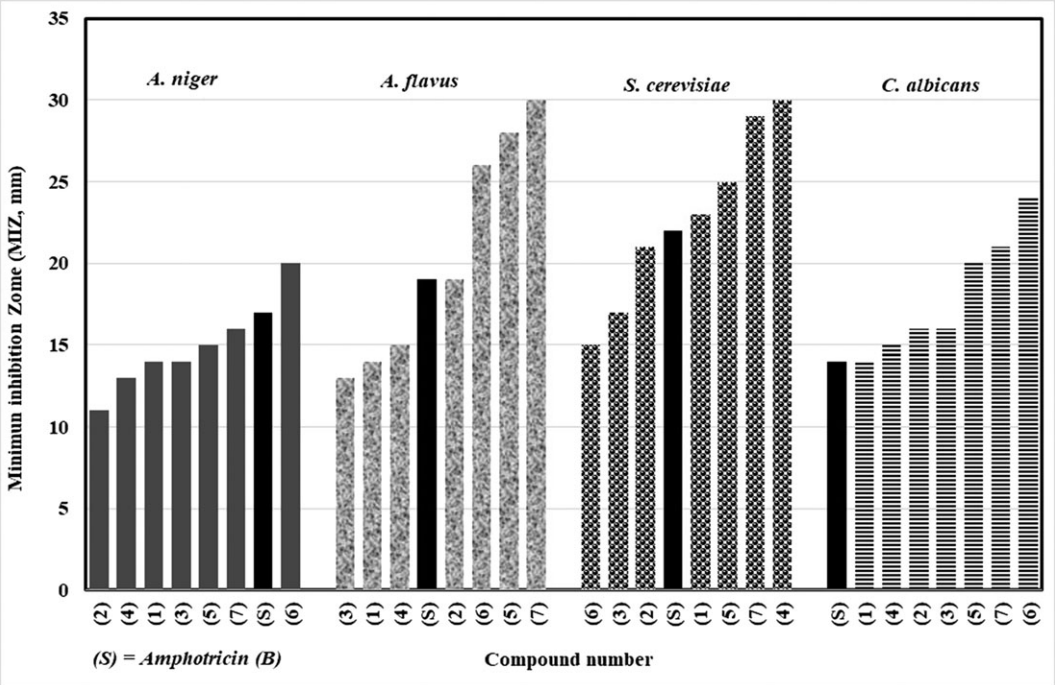

FIGURE 6 The fungicide activity order for the ligand and its complexes against *A. niger, A. Flavus, S. cerevisiae* and *C. albicans*

5 | CONCLUSION

A series of VO^{2+}, Co^{2+}, Ni^{2+}, Cu^{2+}, and Zn^{2+} complexes (Schiff base parent ligand) prepared under mild conditions. The Schiff base and the new six complexes have been characterized by using different analytical and spectroscopic techniques. The entire spectroscopic and analytic data revealed that the Schiff base **(1)** combined with the metal ions as a neutral or as a monobasic tridentate ligand via azomethine nitrogen, ketonic carbonyl oxygen atoms and protonated/deprotonated phenolic hydroxyl group that give finally an octahedral or distorted octahedral geometry. The antifungal screening assignment were tested for the whole synthesized compounds against *A. niger, A. Flavus, S. cerevisiae and C. albicans*. The resulted data displayed that, the whole compounds had a positive activity towards many fungi under study particularly *C. albicans*. While only complex **(6)** showed a good antifungal activity against *A. niger* with MIZ, mm (IA%) equal 20 (117.6%), even as complexes **(5–7)** showed also a well satisfying biological activity against *A. Falvus* with MIZ, mm (IA%) 28(147.4), 26(136.8) and 30(157.9) respectively. In contrast compounds **(1), (4–5)** and **(7)** displayed an exceptional good result against *S. cerevisiae* with MIZ, mm (IA%) 23(104.5), 30(136.3), 25(113.6) and 29(131.8). These results encourage our teamwork to continue preparing more complexes from a Schiff base with a 4,5,6,7-tetrahydrothieno[2,3-c] pyridine moiety in the future.

ORCID

Mohamad M.E. Shakdofa http://orcid.org/0000-0003-0399-1658
Ammar A. Labib http://orcid.org/0000-0002-1564-3477
Naglaa A. Abdel-Hafez http://orcid.org/0000-0003-2211-8088
Hanan A. Mousa http://orcid.org/0000-0001-6373-4552

REFERENCES

[1] K. Brodowska, E. Łodyga-Chruścińska, *Chemik* **2014**, *68*, 129.

[2] H. Schiff, *Justus Liebigs Ann. Chem.* **1864**, *131*, 118.

[3] A. M. Abu-Dief, I. M. A. Mohamed, *Beni-suef Uni. J. Basic and Appl. Sci.* **2015**, *4*, 119.

[4] C. M. da Silva, D. L. da Silva, L. V. Modolo, R. B. Alves, M. A. de Resende, C. V. B. Martins, Â. de Fátima, *J. Adv. Res.* **2011**, *2*(1), 1.

[5] W. A. Zoubi, *Int. J. Org. Chem.* **2013**, *3*, 24.

[6] J. Lewiński, D. Prochowicz, in *Assemblies Based on Schiff Base Chemistry*, (Ed: J. L. Atwood), Elsevier, Oxford **2017**.

[7] F. Sevgi, U. Bagkesici, A. N. Kursunlu, E. Guler, *J. Mol. Struct.* **2018**, *1154*, 256.

[8] E. S. A. El-Samanody, S. A. AbouEl-Enein, E. M. Emara, *Appl. Organomet. Chem.* **2018**, *32*, e4262.

[9] N. Süleymanoğlu, R. Ustabaş, Ş. Direkel, Y. B. Alpaslan, Y. Ünver, *J. Mol. Struct.* **2017**, *1150*, 82.

[10] S. S. Thakkar, P. Thakor, A. Ray, H. Doshi, V. R. Thakkar, *Bioorg. Med. Chem.* **2017**, *25*, 5396.

[11] C. M. da Silva, M. M. Silva, F. S. Reis, A. L. T. G. Ruiz, J. E. de Carvalho, J. C. C. Santos, I. M. Figueiredo, R. B. Alves, L. V. Modolo, Â. de Fátima, *J. Photochem. Photobiol. B Biol.* **2017**, *172*, 129.

[12] B. Iftikhar, K. Javed, M. S. U. Khan, Z. Akhter, B. Mirza, V. McKee, *J. Mol. Struct.* **2018**, *1155*, 337.

[13] S. Tariq, F. Avecilla, G. P. Sharma, N. Mondal, A. Azam, J. Saudi, *Chem. Soc.* **2018**, *22*, 306.

[14] P. H. Wang, J. G. Keck, E. J. Lien, M. M. C. Lai, *J. Med. Chem.* **1990**, *33*, 608.

[15] S. M. Emam, S. A. Abouel-Enein, F. I. Abouzayed, *Appl. Organomet. Chem. 0*, e4073.

[16] Z. Faghih, A. Neshat, A. Wojtczak, Z. Faghih, Z. Mohammadi, S. Varestan, *Inorg. Chim. Acta* **2018**, *471*, 404.

[17] A. M. Gouda, H. A. El-Ghamry, T. M. Bawazeer, T. A. Farghaly, A. N. Abdalla, A. Aslam, *Eur. J. Med. Chem.* **2018**, *145*, 350.

[18] M.-J. Niu, Z. Li, G.-L. Chang, X.-J. Kong, M. Hong, Q.-f. Zhang, *PLoS One* **2015**, *10*, e0130922.

[19] K. Venkateswarlu, M. P. Kumar, A. Rambabu, N. Vamsikrishna, S. Daravath, K. Rangan, Shivaraj, *J. Mol. Struct.* **2018**, *1160*, 198.

[20] P. Ghorai, R. Saha, S. Bhuiya, S. Das, P. Brandão, D. Ghosh, T. Bhaumik, P. Bandyopadhyay, D. Chattopadhyay, A. Saha, *Polyhedron* **2018**, *141*, 153.

[21] X. Liu, C. Manzur, N. Novoa, S. Celedón, D. Carrillo, J.-R. Hamon, *Coord. Chem. Rev.* **2018**, *357*, 144.

[22] Z. Beigi, A. H. Kianfar, H. Farrokhpour, M. Roushani, M. H. Azarian, W. A. K. Mahmood, *J. Mol. Liq.* **2018**, *249*, 117.

[23] F. Wu, C.-J. Wang, H. Lin, A.-Q. Jia, Q.-F. Zhang, *Inorg. Chim. Acta* **2018**, *471*, 718.

[24] M. Sedighipoor, A. H. Kianfar, G. Mohammadnezhad, H. Görls, W. Plass, *Inorg. Chim. Acta* **2018**, *476*, 20.

[25] M. M. E. Shakdofa, H. A. Mousa, A. M. A. Elseidy, A. A. Labib, M. M. Ali, A. S. Abd-El-All, *Appl. Organomet. Chem.* **2018**, 32.

[26] F. A. El-Saied, T. A. Salem, S. A. Aly, M. M. E. Shakdofa, *Pharm. Chem. J.* **2017**, *51*, 833.

[27] F. A. El-Saied, A. N. Al-Hakimi, M. A. Wahba, M. M. E. Shakdofa, *Egypt. J. Chem.* **2017**, *60*, 1.

[28] M. M. Shakdofa, A. N. Al-Hakimi, F. A. Elsaied, S. O. Alasbahi, A. M. Alkwlini, *Bull. Chem. Soc. Ethiop.* **2017**, *31*, 75.

[29] A. G. E. S. Amr, N. A. S. Abdel-Hafez, S. F. Mohamed, M. M. Abdalla, *Turk. J. Chem.* **2009**, *33*, 421.

[30] M. Fujita, T. Seki, H. Inada, N. Ikeda, *Bioorg. Med. Chem. Lett.* **2002**, *12*, 1607.

[31] A. I. Vogel, in *Vogel's textbook of quantitative chemical analysis*, (Eds: G. H. Jeffery, A. I. Vogel), Longman Scientific & Technical, Harlow, Essex, England **1989**.

[32] F. J. Welcher, *The analytical uses of Ethylenedamine Tetraacetic Acid*, D. Van Nostrand Company, Inc, Princeton, New Jersey, USA, **1958**.

[33] G. Svehla, *Vogel's textbook of macro and semi micro Quantitative inorganic analysis*, Longman Inc., New York **1979**.

[34] Z. Holzbecher, L. Divis, M. Kral, L. Sucha, F. Vracil, *Handbook of Organic Reagents in Inorganic Analysis*, Ellis Horwood Press, John Wiley & Sons INC, New York **1976**.

[35] E. A. Du Toit, M. Rautenbach, *J. Microbiol. Methods* **2000**, *42*, 159.

[36] J. G. Collee, T. J. Mackie, J. E. McCartney, '*Mackie & McCartney practical medical microbiology*', Churchill Livingstone, New York, **1996**.

[37] M. Balouiri, M. Sadiki, S. K. Ibnsouda, *J. Pharmaceut. Analy.* **2016**, *6*, 71.

[38] I. A. Holder, S. T. Boyce, *Burns* **1994**, *20*, 426.

[39] R. R. Zaky, K. M. Ibrahim, I. M. Gabr, *Spectrochim. Acta Part A Mol. Biomol. Spectrosc.* **2011**, *81*, 28.

[40] W. J. Geary, *Coord. Chem. Rev.* **1971**, *7*, 81.

[41] S. Naskar, S. Naskar, S. Mondal, P. K. Majhi, M. G. B. Drew, S. K. Chattopadhyay, *Inorg. Chim. Acta* **2011**, *371*, 100.

[42] B. Mustafa, S. Satyanarayana, J. Korean, *Chem. Soc.* **2010**, *54*, 687.

[43] A. S. El-Tabl, *Transit. Met. Chem.* **2002**, *27*, 166.

[44] A. S. El-Tabl, *Transit. Met. Chem.* **1997**, *22*, 400.

[45] Z. H. A. El-Wahab, M. M. Mashaly, A. A. Salman, B. A. El-Shetary, A. A. Faheim, *Spectrochim. Acta Part A Mol. Biomol. Spectrosc.* **2004**, *60*, 2861.

[46] S. P. Dash, S. Pasayat, H. R. D. Saswati, S. Das, R. J. Butcher, R. Dinda, *Polyhedron* **2012**, *31*, 524.

[47] K. Nakamoto, *Infrared and Raman Spectra of Inorganic and Coordination Compounds Part B: Applications in Coordination, Organometallic, and Bioinorganic Chemistry*, John Wiley & Sons INC, New York, **2009**.

[48] A. S. El-Tabl, M. M. E. Shakdofa, M. A. Whaba, *Spectrochim. Acta Part A Mol. Biomol. Spectrosc.* **2015**, *136*, 1941.

[49] F. A. El-Saied, M. M. E. Shakdofa, A. S. El-Tabl, M. M. A. Abd-Elzaher, *Main Group Chem.* **2014**, *13*, 87.

[50] E. Yousif, A. Majeed, K. Al-Sammarrae, N. Salih, J. Salimon, B. Abdullah, *Arab. J. Chem.* **2017**, *10*, S1639.

[51] G. Yeğiner, M. Gülcan, S. Işık, G. Ö. Ürüt, S. Özdemir, M. Kurtoğlu, *J. Fluoresc.* **2017**, *27*, 2239.

[52] A. N. M. A. Alaghaz, H. A. Bayoumi, Y. A. Ammar, S. A. Aldhlmani, *J. Mol. Struct.* **2013**, *1035*, 383.

[53] Ş. Bitmez, K. Sayin, B. Avar, M. Köse, A. Kayraldiz, M. Kurtoɔlu, *J. Mol. Struct.* **2014**, *1076*, 213.

[54] P. B. Sreeja, M. R. P. Kurup, *Spectrochim. Acta Part A Mol. Biomol. Spectrosc.* **2005**, *61*, 331.

[55] Y. Dong, R. K. Narla, E. Sudbeck, F. M. Uckun, *J. Inorg. Biochem.* **2000**, *78*, 321.

[56] A. B. P. Lever, *Inorganic electronic spectroscopy*, Elsevier Science, Amsterdam **1984**.

[57] J. Costa Pessoa, I. Cavaco, I. Correia, I. Tomaz, T. Duarte, P. M. Matias, *J. Inorg. Biochem.* **2000**, *80*, 35.

[58] A. A. A. Emara, A. A. Saleh, O. M. I. Adly, *Spectrochim. Acta Part A Mol. Biomol. Spectrosc.* **2007**, *68*, 592.

[59] J. W. Lai, C. W. Chan, C. H. Ng, I. H. Ooi, K. W. Tan, M. J. Maah, S. W. Ng, *J. Mol. Struct.* **2016**, *1106*, 234.

[60] S. Chandra, S. Bargujar, R. Nirwal, N. Yadav, *Spectrochim. Acta Part A Mol. Biomol. Spectrosc.* **2013**, *106*, 91.

[61] M. M. Al-Ne'aimi, M. M. Al-Khuder, *Spectrochim. Acta Part A Mol. Biomol. Spectrosc.* **2013**, *105*, 365.

[62] G. R. Hanson, T. A. Kabanos, A. D. Keramidas, D. Mentzafos, A. Terzis, *Inorg. Chem.* **1992**, *31*, 2587.

[63] A. S. El-Tabl, M. M. E. Shakdofa, A. M. E. Shakdofa, *J. Serb. Chem. Soc.* **2013**, *78*, 39.

[64] S. S. Dodwad, R. S. Dhamnaskar, P. S. Prabhu, *Polyhedron* **1989**, *8*, 1748.

[65] N. Raman, Y. Pitchaikani Raja, A. Kulandaisamy, *Proc. Indian Acad. Sci. (Chem. Sci.)* **2001**, *113*, 183.

[66] M. Patron, D. Kivelson, R. N. Schwartz, *J. Phys. Chem.* **1982**, *86*, 518.

[67] F. A. Walker, R. L. Carlin, P. H. Rieger, *J. Chem. Phys.* **1966**, *45*, 4181.

[68] B. R. McGarvey, E. L. Tepper, *Inorg. Chem.* **1969**, *8*, 498.

[69] B. J. Hathaway, D. E. Billing, *Coord. Chem. Rev.* **1970**, *5*, 143.

[70] D. R. Brown, D. X. West, *J. Inorg. Nucl. Chem.* **1981**, *43*, 1017.

[71] K. Nagashri, J. Joseph, C. J. Dhanaraj, *Appl. Organomet. Chem.* **2011**, *25*, 704.

[72] A. A. G. Tomlinson, B. J. Hathaway, *J. Chem. Soc. A: Inorg. Phys. Theo.* **1685**, *1968*.

[73] A. S. El-Tabl, F. A. Aly, M. M. E. Shakdofa, A. M. E. Shakdofa, *J. Coord. Chem.* **2010**, *63*, 700.

[74] A. N. Al-Hakimi, A. S. El-Tabl, M. M. E. Shakdofa, *J. Chem. Res.* **2009**, *770*.

[75] D. Kivelson, R. Neiman, *J. Chem. Phys.* **1961**, *35*, 149.

[76] N. A. Mangalam, M. R. Prathapachandra Kurup, *Spectrochim. Acta Part A Mol. Biomol. Spectrosc.* **2011**, *78*, 926.

[77] N. M. Shauib, A. Z. A. Elassar, A. El-Dissouky, *Spectrochim. Acta Part A Mol. Biomol. Spectrosc.* **2006**, *63*, 714.

[78] R. K. Ray, G. B. Kauffmann, *Inorg. Chim. Acta* **1990**, *174*, 237.

[79] R. K. Ray, G. B. Kauffman, *Inorg. Chim. Acta* **1990**, *174*, 257.

[80] A. S. El-Tabl, *Pol. J. Chem.* **1997**, *71*, 1213.

[81] B. Swamy, J. R. Swamy, *Transit. Met. Chem.* **1991**, *16*, 35.

[82] B. S. Creaven, B. Duff, D. A. Egan, K. Kavanagh, G. Rosair, V. R. Thangella, M. Walsh, *Inorg. Chim. Acta* **2010**, *363*, 4048.

[83] M. Tümer, H. Köksal, M. K. Sener, S. Serin, *Transit. Met. Chem.* **1999**, *24*, 414.

[84] B. G. Tweedy, *Phytopathology* **1964**, *55*, 910.

How to cite this article: Shakdofa MME, Labib AA, Abdel-Hafez NA, Mousa HA. Synthesis and Characterization of VO^{2+}, Co^{2+}, Ni^{2+}, Cu^{2+} and Zn^{2+} Complexes of a Schiff base ligand derived from ethyl 2-amino-6-ethyl-4,5,6,7-tetrahydrothieno[2,3-c]pyridine-3-carboxylate and their Investigation as fungicide Agents. *Appl Organometal Chem*. 2018; e4581. https://doi.org/10.1002/aoc.4581